Formation of cholesterol monohydrate crystals in macrophage-derived foam cells

Rajendra K. Tangirala,* W. Gray Jerome,† Nancy L. Jones,† Donald M. Small,§ William J. Johnson,* Jane M. Glick,* Florence H. Mahlberg, and George H. Rothblat[1,*]**

Department of Biochemistry,* Medical College of Pennsylvania, 2900 Queen Lane, Philadelphia, PA 19129-1121; Department of Pathology,† Bowman Gray School of Medicine, Winston-Salem, NC 27157; Department of Biophysics,§ Boston University School of Medicine, Boston, MA 02118; and Department of Molecular Cardiology,** Lederle-American Cyanamid, Pearl River, NY 10965

Abstract In a previous study using the J774 macrophage foam cells, we quantitated the accumulation of unesterified (free) cholesterol derived from cholesteryl ester hydrolysis in lysosomes, after phagocytic uptake of cholesteryl ester droplets. In the present study, we examined whether the accumulation of free cholesterol in lysosomes leads to the formation of cholesterol monohydrate crystals by analyzing the lipid composition of low density lysosome fractions isolated from cholesteryl ester-loaded macrophages after a 24-h incubation. Phase diagrams of the constituent lipids in the lipid-filled lysosomes predicted the formation of cholesterol monohydrate crystals. The formation of cholesterol monohydrate crystals was observed in cholesteryl ester-loaded macrophages after a 48-h incubation by polarizing light microscopy. The crystals had a density of 1.04 g/ml and the morphology of cholesterol monohydrate crystals with an acute edge angle of about 80°. The crystals appeared as needles as well as plates and melted only when heated to greater than 85°C. The physical properties of these crystals are characteristic of cholesterol monohydrate. In our studies, crystal formation was observed even when cells had active acyl-CoA:cholesterol acyltransferase or when cholesterol efflux was stimulated. Electron microscopy and acid phosphatase cytochemistry of lysosomes in cholesteryl ester-loaded cells confirmed that cholesterol crystal formation occurred within lipid-loaded lysosomes. Time-lapse video microscopic studies revealed that most of the cells containing cholesterol monohydrate crystals not only remain viable but also have the capacity to translocate single crystals within cells. The data demonstrate that lysosomal accumulation of free cholesterol in macrophages after phagocytic uptake and hydrolysis of cholesteryl ester droplets leads to the formation of cholesterol monohydrate crystals within lipid-filled lysosomes. Such a process may lead to deposition of free cholesterol and cholesterol monohydrate crystals in macrophage foam cells during the progression of atherosclerosis.—**Tangirala, R. K., W. G. Jerome, N. L. Jones, D. M. Small, W. J. Johnson, J. M. Glick, F. H. Mahlberg, and G. H. Rothblat.** Formation of cholesterol monohydrate crystals in macrophage-derived foam cells. *J. Lipid Res.* 1994. **35:** 93–104.

Supplementary key words lysosomes • J774 macrophage foam cell

During the progression of atherosclerotic lesions, increasing amounts of both esterified and unesterified (free) cholesterol (FC) accumulate within foam cells of both macrophage and smooth muscle cell origin (1–3). In early lesions, the cholesterol in foam cells is present primarily as cytoplasmic cholesteryl ester (CE) droplets (4, 5). However, as the lesion progresses there appears to be an increasingly greater involvement of lysosomes as a site for cholesterol accumulation (5–7), and an appreciable portion of the cholesterol within these lysosomes is present as free cholesterol (8). As a lesion develops into advanced plaque, a necrotic core becomes evident and an increasing number of crystals become apparent (9, 10). The origin of these crystals remains obscure, and it has been suggested that they may arise from either intracellular (10–12) or extracellular processes (13, 14).

Previous studies from our laboratory have documented that both macrophage and smooth muscle cells can incorporate CE inclusions by phagocytosis (15–17). Using a J774 macrophage foam cell model, we have recently investigated the accumulation of FC derived from CE hydrolysis in lysosomes, after phagocytic uptake of CE droplets (18). FC accumulation in lysosomes was independent of cholesterol esterification by acyl-CoA:cholesterol acyltransferase (ACAT) and was not influenced by the stimulation of cholesterol efflux (18). FC deposition in the lysosomes increased in proportion to the extent of CE droplet uptake and with the time of incubation. The chemical analysis of the low density lysosome fraction isolated 24 h after CE-lipid droplet uptake suggested that the lipid composition

Abbreviations: ACAT, acyl-CoA:cholesterol acyltransferase; BSA, bovine serum albumin; β-VLDL, β-very low density lipoprotein; CE, cholesteryl ester; EtBr, ethidium bromide; FBS, fetal bovine serum; FC, free (unesterified) cholesterol; HDL, high density lipoprotein; LDH, lactate dehydrogenase; LDL, low density lipoprotein; MPM, mouse peritoneal macrophages; NADH, nicotinamide adenine dinucleotide; PBS, phosphate-buffered saline; PC, phosphatidylcholine; PL, phospholipid; SMC, smooth muscle cells; DIC, differential interference contrast; TLC, thin-layer chromatography.

[1]To whom correspondence should be addressed.

was such that a portion of the FC should be present as cholesterol crystals (10). Based on the prediction from the phase diagram of the component lipids (10, 19), we extended the incubation period after the phagocytic uptake of CE inclusions to periods longer than 24 h. Light and electron micrographic examination of these cells demonstrated the presence of large numbers of crystals, which we have now identified as cholesterol monohydrate. The conditions leading to their formation, the intracellular location of the crystals, and their effect on the cells have been investigated. The availability of a cell culture system that promotes the formation of intracellular cholesterol crystals provides an opportunity to study the events that could result in the deposition of crystals in the advanced atherosclerotic plaque.

MATERIALS AND METHODS

Materials

Unless otherwise stated, the materials used were the same as those reported previously (18). Sodium pyruvate solution was obtained from Mediatech, Washington, DC. β-Nicotinamide adenine dinucleotide (reduced form), ethylene glycol monomethyl ether, β-glycerophosphate, and ethidium bromide (2,7-diamino-10-ethyl-9-phenanthridinium bromide) were purchased from Sigma Chemical Co., St. Louis, MO. Chemicals used for electron microscopy were obtained from Electron Microscopy Sciences, Ft. Washington, PA. Lead nitrate was obtained from Fisher Scientific Co., Pittsburgh, PA.

Cell cultures

Murine J774 macrophages maintained in RPMI 1640 supplemented with 10% FBS were plated on glass coverslips as described previously (18). Thioglycollate-elicited mouse peritoneal macrophages were isolated from B6C3F1 mice and plated as described by Bernard et al. (20). Two hours after plating, the adherent cells were rinsed extensively and loaded as described in the following section.

Preparation of cholesteryl oleate droplets and cholesterol acceptor particles

Anisotropic cholesteryl oleate droplets used for loading cells, and apoHDL/phosphatidylcholine (apoHDL/PC) complexes used in efflux experiments were prepared as described previously (18).

Lipid loading and conditions for the incubation of CE-loaded cells

Confluent monolayers of cells grown on glass coverslips (35 × 35 mm) in 60-mm Petri plates were loaded for 3 h with lipid droplets containing cholesteryl oleate using an inverted culture technique (15). However, where stated, in some experiments loading with CE droplets was extended to 24 h to enhance FC crystal formation. After loading, the cells were rinsed with serum-free RPMI and incubated further for up to 72 h in RPMI medium supplemented with either 1% BSA or 1% FBS. Most incubations were carried out in the presence of the ACAT inhibitor, Sandoz 58035 (2 μg/ml); however, for some experiments, CE-loaded cells were incubated in the absence of 58035 and/or in the presence of a cholesterol acceptor, apoHDL/PC complexes (200 μg PC/ml). In cell viability experiments, both non-loaded (control) cells and cells loaded with CE droplets were incubated in RPMI medium supplemented with 1% FBS for up to 96 h.

Isolation of lipid fractions containing lysosomes

After the indicated incubations, cells were homogenized and a floating lipid fraction containing lipid-filled lysosomes was separated from a pellet fraction enriched with cell membranes, using centrifugation conditions as previously described (18).

Determination of cell viability by the release of lactate dehydrogenase (LDH)

Cell viability was assessed by LDH release from cells. Parallel sets of cells loaded with CE-droplets and control cells not loaded with CE were incubated in medium supplemented with 1% FBS for 96 h. After 0, 24, 48, 72, and 96 h of incubation, the media were collected and centrifuged at 1000 rpm (Sorvall RT 6000) for 10 min at room temperature to pellet any floating cells. Cells from the plates were harvested into 0.05 M potassium phosphate buffer (pH 7.4) and were sonicated for 10 min on ice. LDH activity in 100-μl aliquots of media and cell lysates were measured as described by Bernstein and Everse (21). The LDH activity in the medium represented the activity released from cells. The values for LDH in the medium when combined with the LDH values for cell lysates gave total LDH values. The release of LDH to the medium is expressed as the percent of total LDH activity.

The viability of CE-loaded cells containing cholesterol crystals was also assessed by an ethidium bromide (EtBr) exclusion method (22). In this method, the cells were rinsed with PBS and examined under UV-light using a Leitz inverted fluorescent microscope immediately after the addition of PBS containing ethidium bromide (6 μg/ml). Nuclei in damaged or leaky cells were stained bright orange under UV-light, while the intact cells excluded EtBr and remained nonfluorescent.

Biochemical analyses

The masses of free and esterified cholesterol in lipid fractions containing lysosomes and pellet fractions were calculated based on the specific activities of the radiolabeled CE supplied to the cells, as described previously

(18). All other analytical procedures were conducted as previously reported (18).

Crystals from CE-loaded cells were isolated using sucrose density gradient centrifugation. Cell homogenates placed on sucrose density gradient with densities ranging from 1.015 to 1.082 g/ml were centrifuged at 100,000 *g* for 1 h at 20°C in a Beckman SW 27 rotor (Beckman Instruments Inc, Palo Alto, CA). Crystals sedimented to a density of 1.040 g/ml.

Microscopy

The occurrence of crystals was quantitated in cells loaded with CE droplets for 24 h and further incubated in medium containing 1% BSA for periods ranging from 12 to 48 h. Coverslips were then transferred onto microscopic slides, and examined at high resolution using an Olympus BH2 photo microscope equipped with phase Nomarski and polarizing optics. To quantify crystal formation, 15 arbitrarily selected fields were examined by Nomarski differential interference contrast (DIC) optics and the percentage of cells containing FC crystals was determined at each time point. The presence of crystals identified by DIC was confirmed by polarizing microscopy.

In the cell preparations the crystals were oriented in many directions and estimates of crystal morphology were difficult. Therefore, coverslips with cells attached were scraped, minced, and a drop of water was added. Coverslips were then mounted with glycerol–water 50:50 (v/v) and observed. This process allowed some of the crystals to lie flat on the surface of the slide where their morphology could be examined and their melting characteristics could be established using a hot stage microscope.

Video light microscopy was used to study the behavior of cells after crystal formation. Coverslips of lipid-loaded cells were placed in a Sykes-Moore chamber (Bellco, Vineland, NJ) and mounted on the stage of a Zeiss IM35 inverted microscope equipped with a Hamamatsu Nouvicon video camera. RPMI medium was replaced with HEPES-buffered RPMI. The microscope stage was maintained at 37°C using an Opti-quip infrared incubator (Opti-Quip Inc., Highland Mills, NY). Time-lapse images were recorded using a Panasonic JVC 9000 super VHS time-lapse recorder. The principal mode of operation was Allen video-enhanced contrast-DIC (23), but polarizing and phase optics also were selectively used to analyze the crystals. Cells with crystals were recorded and their behavior was observed from digital records of the cultures for periods ranging from 2 to 24 h.

Microscopic quantitation of lipid deposition was carried out by using electron microscopy as previously described (24). The intracellular location of crystals was also determined by electron microscopy. Macrophages were treated as described above to maximize crystal formation. Cell cultures were then quickly washed at room temperature with 0.1 M cacodylate buffer (pH 7.2), fixed in cacodylate buffer with 4% glutaraldehyde, washed, and stained to demonstrate the presence of lysosomes by acid phosphatase staining using a modification (24) of Gomori lead precipitation method (25). After incubation the cells were postfixed in 1% osmium tetroxide, scraped from the dish, and embedded as a pellet in epoxy resin. Thin sections of the embedded material were viewed using a Phillips EM 400 electron microscope. As a cytochemical control, some cells were incubated in reaction mixture that lacked substrate.

RESULTS

Using the J774 macrophage foam cell model, we have demonstrated previously the accumulation of FC in lipid-filled lysosomes after phagocytosis and lysosomal hydrolysis of CE droplets (18). A substantial fraction (20–30%) of FC generated by CE hydrolysis accumulated in the lipid-filled, low density lysosomes (18). In the present study, we examined whether the accumulation of FC in lysosomes leads to formation of cholesterol monohydrate crystals. To further characterize the physical behavior of FC present in these lysosomes, as well as cholesterol in the pellet fractions containing the bulk of the plasma membranes, J774 cells, loaded with CE-droplets and subsequently incubated for 24 h, were homogenized and the fractions were isolated as described in Methods. The lipid composition of the fractions was determined, and the relative weight percents of three major lipids, FC, CE, and PL are presented in **Table 1.** As expected, a large fraction of lipid in the pellet was phospholipid (ranging from 69.7 to 80.0 wt%). The pellet fraction contained 98% of the total plasma membrane enzyme marker activity as previously observed (18). Cholesteryl ester in the pellet represented only 2.3 to 4.0 wt%, while FC was present at 18.0 to 26.0 wt%. As the maximum solubility of FC and CE in the phospholipid bilayer phase are 33 and 5 wt%, respectively (10, 19), the relative proportions of FC and CE present in the pellet fraction were within their maximum solubility limits in a phospholipid bilayer. In contrast, the floating lipid fraction containing lysosomes had a greater proportion of lipid as CE (72.0 to 76.2 wt%) and a much smaller proportion of phospholipid (2.2 to 7.6 wt%). Consistent with our previous observations that FC accumulates in lipid-filled lysosomes, a substantial proportion of the lipid in this fraction was FC (17.6 to 22.1 wt%) (Table 1). This level of FC is in excess of its solubility considering the limited FC solubility in CE (maximum solubility 5% (10)) and the low proportion of PL present in this fraction. At concentrations beyond the solubility limits, FC should crystallize, leading to the formation of cholesterol monohydrate crystals (10). Thus, to predict the physical state of lipid phases present in the fractions containing lipid-filled lysosomes as well as in the

TABLE 1. Relative content of cholesteryl ester (CE), free cholesterol (FC), and phospholipid (PL) in the floating lipid and pellet fractions isolated from CE-loaded J774 macrophages after a 24-h incubation

Incubation Conditions	Lipid Fractions Weight %			FC/PL Ratio	Pellet Fractions Weight %			FC/PL Ratio
	FC	CE	PL		FC	CE	PL	
No acceptor + S 58035 (n = 3)	22.1 (± 5.8)	72.4 (± 5.1)	5.5 (± 0.9)	4.2 (± 1.8)	26.3 (± 3.4)	4.0 (± 0.5)	69.7 (± 3.3)	0.3 (± 0.1)
+ Acceptor + S 58035	21.7	76.2	2.2	10.0	18.0	2.3	79.7	0.2
+ Acceptor No S 58035 (n = 2)	17.6	74.8	7.6	2.6	18.2	2.7	79.1	0.2
No acceptor No S 58035 (n = 3)	18.2 (± 2.3)	76.2 (± 1.2)	5.6 (± 3.4)	4.6 (± 3.5)	21.9 (± 2.1)	3.7 (± 0.9)	74.4 (± 2.1)	0.3 (± 0.1)

Confluent J774 macrophages were loaded with sonicated cholesteryl oleate droplets (133 μg esterified cholesterol/ml) for 3 h using an inverted culture technique. After further incubation for 24 h in RPMI under the indicated conditions, the cells were homogenized and the floating lipid fractions containing lipid-filled lysosomes and the pellet fractions were obtained by ultracentrifugation of cell homogenates as described in Methods. The lipid isolated from the fractions was separated into free and esterified cholesterol and the masses were determined using specific activity of radiolabel. Phospholipid mass was estimated from the determination of phospholipid-phosphorus. Acceptor, apoHDL/phosphatidylcholine complexes (200 μg PL/ml); S 58035, ACAT inhibitor, Sandoz 58035 (2 μg/ml).

pellet fractions, the compositional data determined from these fractions were plotted on a triangular phase diagram (10). This analysis shows that the lysosomes contain 2.8–3.5 times the amount of FC that can be solubilized at equilibrium. Such high levels of cholesterol predicted the presence of cholesterol monohydrate crystals as one of three lipid phases that would be present in the floating lipid fraction. In contrast, on the phase diagram the points corresponding to the composition of the pellet fractions were in a zone with a single lipid phase, a phospholipid bilayer (10, 19).

In earlier studies on the lysosomal accumulation of FC in J774 cells, we routinely had used a post-loading incubation time of 24 h, and had not observed cholesterol crystals when cells were examined by light or electron microscopy. However, because the lipid phase diagram predicted the presence of crystals, we extended the incubation period to 48 h. Consistent with the prediction, prominent crystals appeared after a 48-h incubation of cells that had been loaded with CE-droplets (**Fig. 1**). Experiments were also conducted to examine the effect of an active ACAT or the stimulation of cholesterol efflux. FC crystals were observed in CE-loaded cells incubated in the presence or absence of the ACAT inhibitor S 58035 (2 μg/ml) or with an extracellular cholesterol acceptor, apoHDL/phosphatidylcholine complexes (200 μg PL/ml). The formation of prominent crystals was also observed when CE-loaded cells were incubated in a medium supplemented with 5% FBS. The lipid composition of the fractions isolated from CE-loaded cells incubated for 24 h in the absence of 58035 (active ACAT) or the presence of extracellular cholesterol acceptor is presented in Table 1.

Following homogenization of CE-loaded cells after 48 h of incubation, the crystals were isolated on a sucrose density gradient by sedimenting them to a density of 1.04 g/ml, which is the density of cholesterol monohydrate crystals (10, 26, 27). The isolated crystalline material moved as free cholesterol on a TLC plate when developed in 100% ethyl ether or petroleum ether–ethyl ether–glacial acetic acid 85:15:1.5 (v/v/v). Cholesteryl ester and phospholipid also appeared as minor lipids on the TLC plate. When cells containing crystals were minced on coverslips and mounted with glycerol–water 50:50 (v/v), the crystals had the classic appearance of cholesterol monohydrate, parallelogram plates with an acute edge angle of about 80°. Crystals did not melt until above 85°C on a hot stage microscope, suggesting that they were not CE crystals (10, 26). However, there was an observable change from crystalline state to a liquid crystalline state between 85 and 92°C. This change in physical state occurs when cholesterol monohydrate undergoes a transition to anhydrous form (10, 26). The physical properties discussed above are characteristic of authentic cholesterol monohydrate crystals (10). Based on these observations, the crystals observed in CE-loaded cells after incubation for 48 h can be identified as cholesterol monohydrate.

Experiments were also conducted to examine whether the cholesterol crystal formation observed in the J774 macrophages also occurred in thioglycollate-elicited mouse peritoneal macrophages (MPM). The MPM were loaded with CE droplets for 3 h using the inverted culture technique, followed by a further incubation in RPMI supplemented with 1% BSA. As in the J774 macrophage foam cell model, prominent crystals were observed in the MPM after a 48-h incubation. Thus, the formation of cholesterol crystals after the phagocytic incorporation and lysosomal CE hydrolysis is apparently not restricted to J774 cells and also occurs in other types of macrophages.

For microscopic quantitation, J774 cells were loaded with CE droplets for 24 h to enhance the formation of

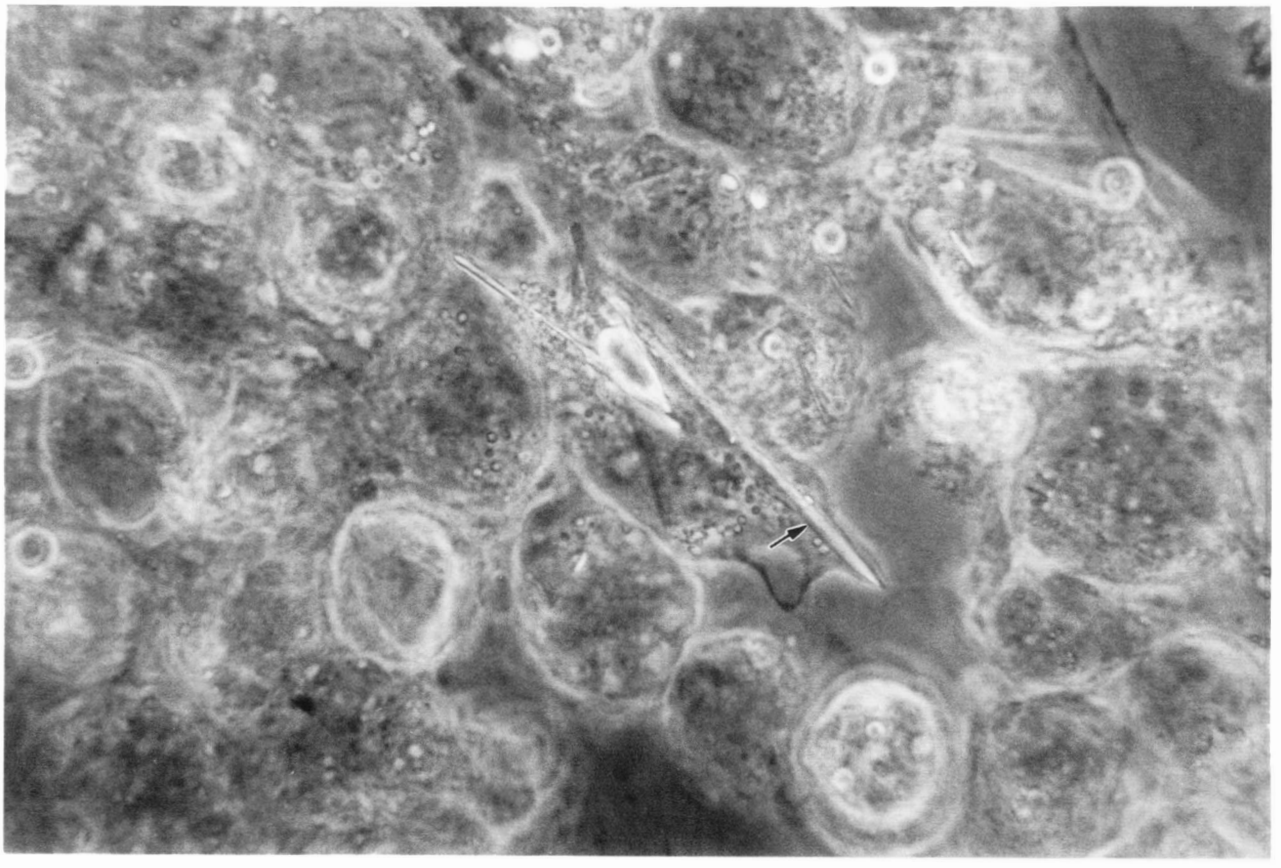

Fig. 1. Phase contrast light micrograph of cells loaded with CE droplets for 3 h and incubated for 48 h in the absence of CE droplets. The central cell contains a prominent cholesterol crystal extending across the cell (arrow). The protrusion of the cell membrane is evident due to the presence of the large crystal within the cell. A few other crystals are also present in the cells.

crystals by increasing loading. After incubation, virtually all cells incubated with CE droplets developed lipid deposits visible by DIC light microscopy. Electron microscopic quantitation of this lipid accumulation revealed that more than 85% of the excess lipid was located within large, swollen lysosomes. However, cells did not contain crystals. **Fig. 2** depicts the averaged results of three representative experiments in which crystal formation was quantified. After loading, the cells were incubated in a medium containing 1% BSA. Generally, after 12 h of incubation a few cells had developed crystals, but the most dramatic increase in crystal formation was seen between 12 and 24 h post-loading. In one experiment 10% of cells developed crystals after 24 h of incubation.

In these experiments there was some variability in the timing and the extent of crystal formation. However, as shown in Fig. 2, there was a general trend with the crystal formation continuing to increase over the entire 48 h of incubation with the percentage of cells with crystals reaching an average of 8% (SD ± 0.35).

Electron microscopic cytochemistry was used to localize the intracellular site of crystal formation (**Fig. 3**). The crystals generally had an elongate shape with apparent rigid sides. At higher magnification, a membrane could be seen surrounding the crystals (Fig. 3, inset). Along the length of crystal, portions of the surrounding membranes were expanded outward and contained debris and acid

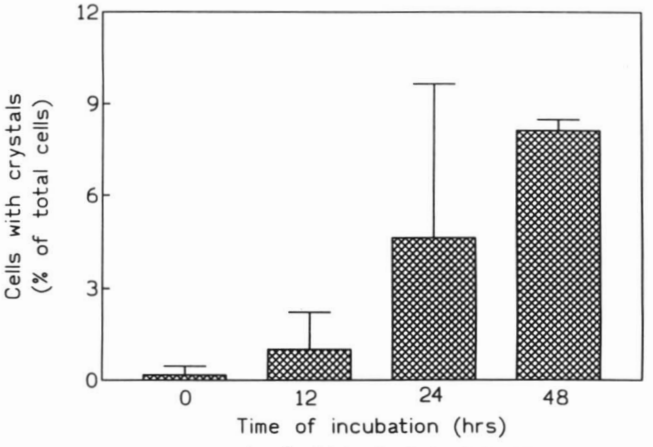

Fig. 2. Effect of incubation for 24 h of cells loaded with CE droplets for 24 h. After loading, medium was replaced with RPMI containing 1% FBS. Fifteen microscopic fields were counted for each time point, and the percentage of cells containing crystals was determined. Each bar represents an average ± SD of three separate experiments.

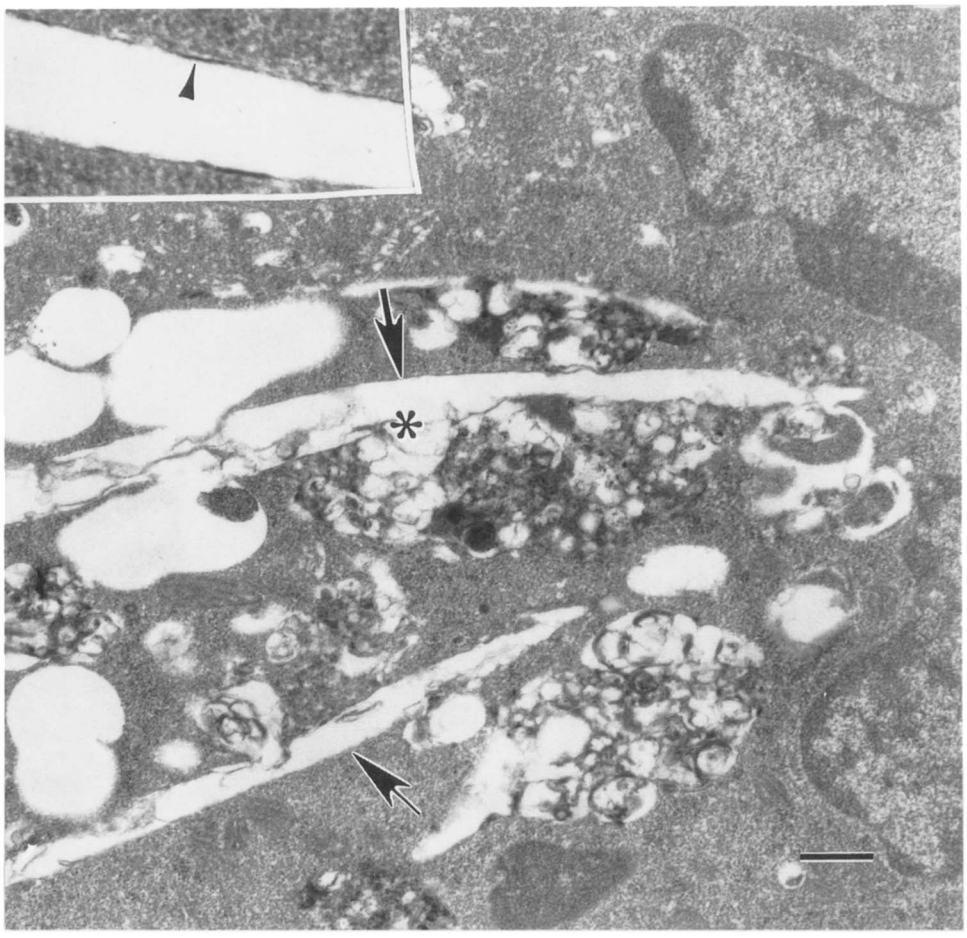

Fig. 3. Electron micrograph of cell incubated with CE droplets for 24 h and then incubated for 48 h in medium containing 1% BSA. Several crystals (arrows) are apparent surrounded by limiting membranes (inset, arrowheads) and associated with areas of acid phosphatase activity (*) indicating the crystals were contained within secondary lysosomes. Magnification, 20,000 ×; bar = 0.5 μm. Inset: Higher magnification of crystal. Magnification, 59,000 ×.

phosphatase reaction product characteristic of secondary lysosomes. Taken together, these observations suggest that cholesterol crystal formation occurred within cholesterol-enriched secondary lysosomes.

The effect of cholesterol monohydrate crystals on cell behavior was monitored by video light microscopy. Time-lapse images showed that cells containing a single crystal remain motile. In addition, the cells had the ability to translocate the crystal within the cytoplasm. This translocation usually took the form of a slow back and forth movement (**Fig. 4**). However, rotation of the crystal along the long axis of the crystal was occasionally noted. In time-lapse, this latter movement was reminiscent of a slow-moving clock hand with the cell acting as the clock face. Although a single crystal appeared to have little effect on cell behavior, cells with three or more crystals invariably had ceased movement, suggesting they were dying (**Fig. 5**). Cell death is also suggested by the absence of extracellular crystals early in the experiments and their appearance in the medium at later time points. An alternate hypothesis to explain the appearance of extracellular crystals is the expulsion of crystals from living cells. Our experiments were unable to differentiate between these two mechanisms. Whichever the explanation, the expulsion did not appear to occur frequently, as we were unable to record it in time-lapse studies of a number of cells containing crystals. This was despite the obvious increase of crystals in the medium with time.

To examine the effect of cholesterol crystal formation on the viability of CE-loaded cells and to compare the viability with non-loaded (control) cells, the release of the cytoplasmic marker enzyme, lactate dehydrogenase (LDH) was determined over 96 h of incubation. As shown in **Fig. 6,** the CE-loaded cells released more LDH than non-loaded cells. In spite of the quantitatively higher LDH release from CE-loaded cells, the rate of LDH release was similar to that of non-loaded cells over the entire 96-h incubation (Fig. 6). In the CE-loaded cells,

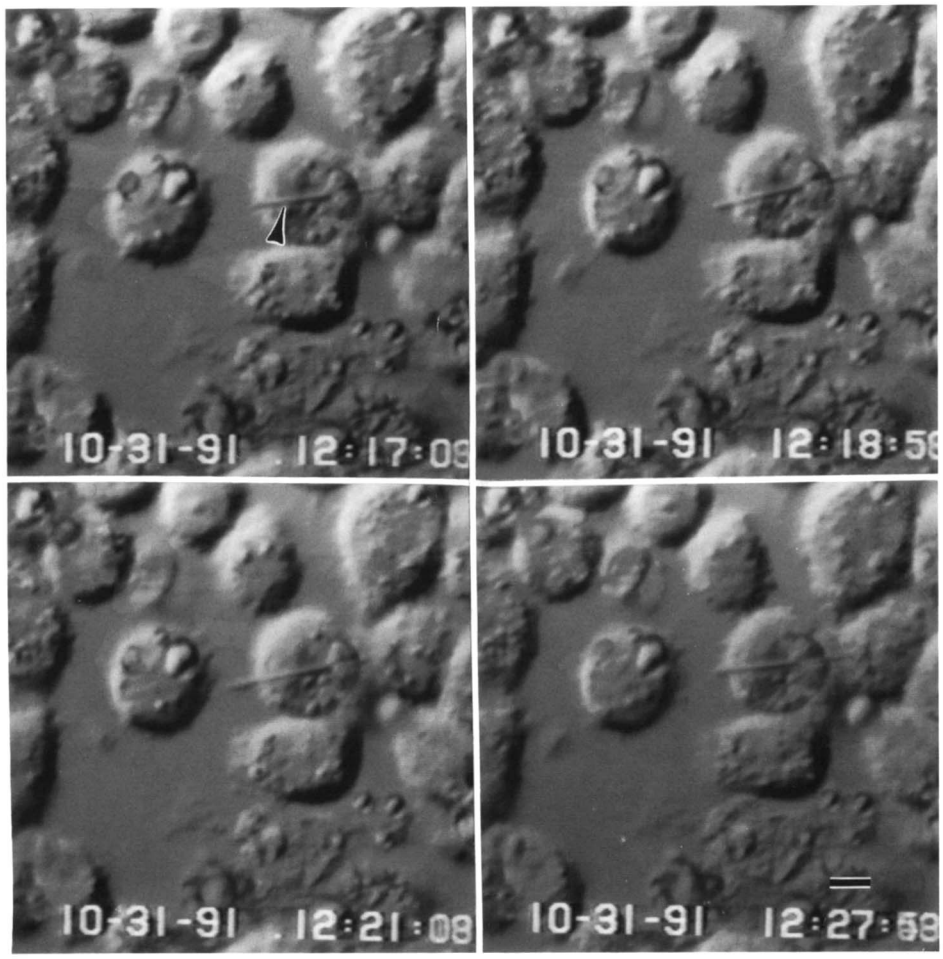

Fig. 4. Four frames from time-lapse video of cholesterol crystal-containing cell. During the 11 min represented here, the cell moves the crystal (arrowhead) first to the left and then back to the right. Magnification, 1,000 ×; bar = 5 μm.

prominent FC crystals were observed after 48 h. In spite of the appearance of these crystals, no overall change in the pattern of LDH release was observed (Fig. 6). Thus, cells containing FC crystals appear to remain viable as indicated by the pattern of LDH release.

As not all cells exhibited crystal formation, it was possible that cell death was confined to a limited number of cells and their death would not significantly increase LDH release. Thus, in addition to monitoring LDH release from cells, the ethidium bromide (EtBr) exclusion method was used to qualitatively assess staining of cells containing FC crystals. After 48 h of incubation, approximately 6% of the cells in the monolayer stained positively with EtBr and there was no evidence that a higher fraction of cells with crystals stained with EtBr. In spite of the presence of prominent FC crystals, most CE-loaded cells remained non-fluorescent when examined under UV-light in the presence of EtBr. A lack of specific EtBr staining of cells containing FC crystals and presence of a similar level of staining in cells without obvious crystals, indicated that most of the cells containing FC crystals remained viable throughout the incubation period.

DISCUSSION

In this study, we demonstrated the formation of cholesterol monohydrate crystals in the J774 macrophage foam cell model in which phagocytic incorporation of CE droplets leads to lysosomal hydrolysis and generation of FC (17). Recently, we quantitatively characterized FC accumulation in a population of low density, lipid-filled lysosomes that were present in such CE-loaded cells. Lysosomal FC accumulation occurs independently of esterification by ACAT or cholesterol efflux (18). We established that 20–40% of the FC liberated upon the hydrolysis of the CE was retained in the lysosomes. Thus, the pool of lysosomal FC increased with both the time of incu-

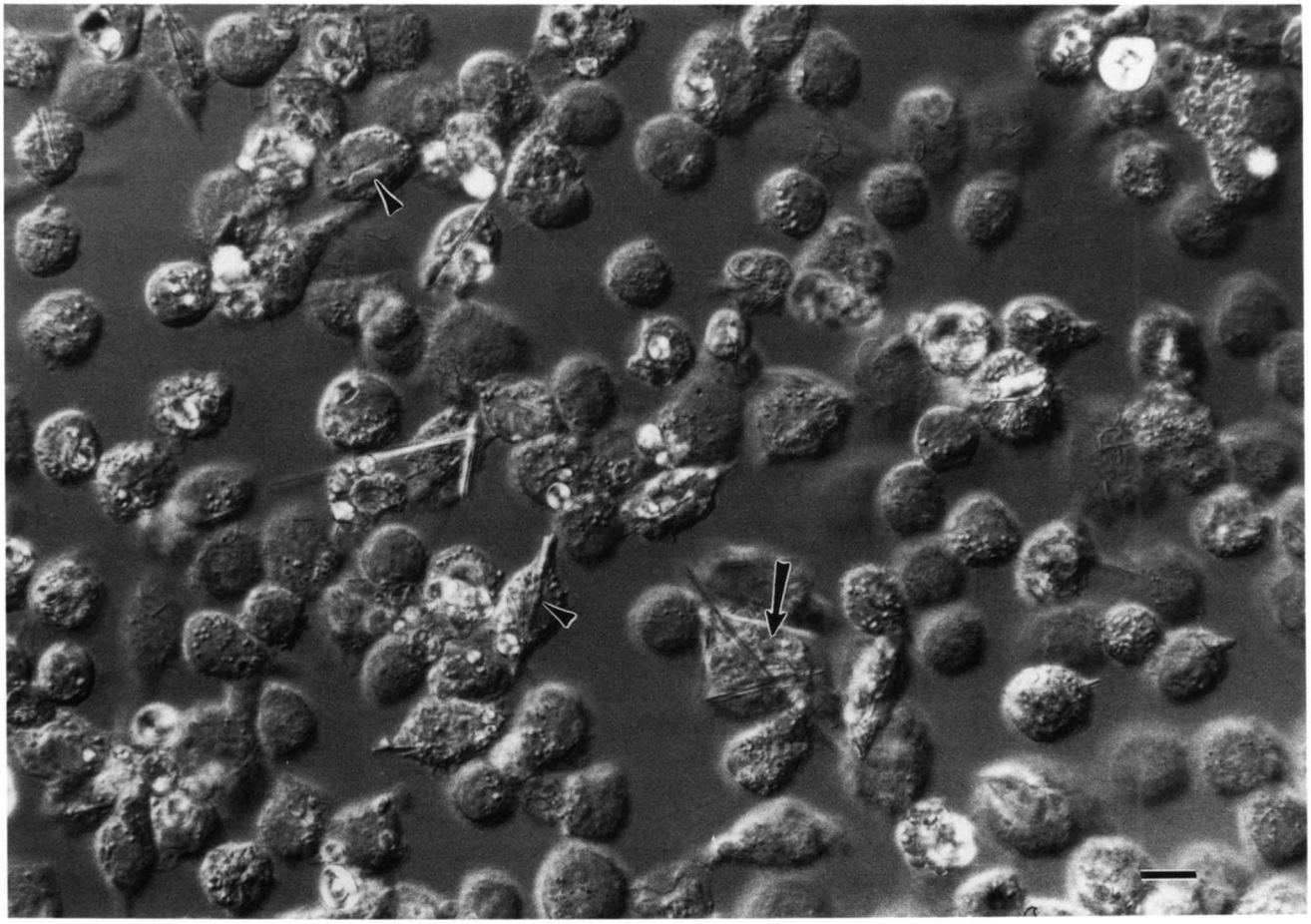

Fig. 5. Nomarski DIC image of cells incubated with CE droplets for 24 h and then incubated for 48 h in medium containing 1% BSA. Several cells (arrowheads) contain single crystals and were motile. However, cells, such as one indicated by the arrow, with multiple crystals usually remained motionless. Magnification, 675 ×; bar = 10 μm.

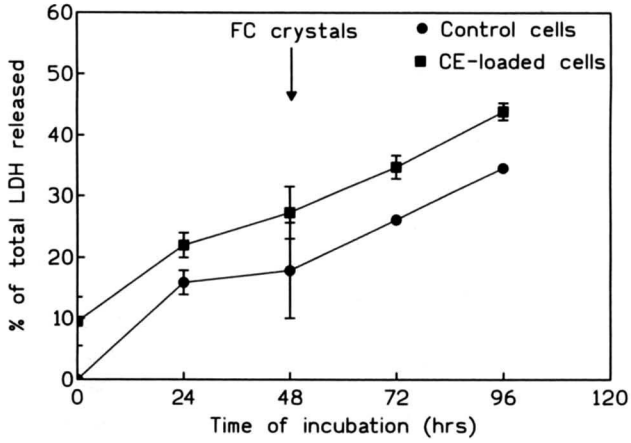

Fig. 6. Release of lactate dehydrogenase (LDH) from CE-loaded and non-loaded (control) J774 macrophages. Confluent monolayers of control J774 cells and cells loaded with CE droplets for 3 h were incubated in RPMI supplemented with 1% FBS for 96 h. After 0, 24, 48, 72, and 96 h, media were removed from triplicate plates and the cell lysates obtained as described in Methods were assayed for LDH activity. Each point represents a mean ± SD of triplicate determinations. When not apparent the SD bars are within the symbols.

bation and increased uptake of CE droplets (18). Although the mechanism(s) responsible for FC accumulation in the lysosomes remain to be resolved, it appears to be a result of rapid hydrolysis of CE coupled with trapping of some of the generated FC within lipid phases of the lysosome. Based on the composition of the lipid layer isolated after 24 h, one would have predicted that some of the FC should be present as crystals. However, such crystals were not evident, suggesting that after 24 h of CE hydrolysis the FC in the lysosomes is in a supersaturated, metastable state. Continued incubation beyond 24 h resulted in the rapid appearance of intracellular crystals (Fig. 1), which were present within lysosomes (Fig. 3). Although extensive observations of cholesterol-loaded cells were conducted using time-lapse video microscopy, we never observed the actual formation of crystals within cells. On a number of occasions a sudden elongation of a lipid droplet was observed, and it is probable that this change in shape of the lipid-loaded lysosomes occurred when the excess FC formed a small crystal. Once a small

FC crystal was present within the lysosome, continued hydrolysis of the CE would lead to the growth of the large crystals illustrated in Figs. 1 and 5. After the appearance of prominent FC crystals, cells appeared to remain viable. The movement of FC crystals within cells that we observed in the time-lapse video microscopy (Fig. 4) indicates that the cells were not only viable but also had the capability to translocate large, single FC crystals. Although the pattern of LDH release and EtBr staining in cells containing FC crystals was essentially similar to that observed in control cells, electron microscopic examination gave the impression that cells that contained multiple crystals often appeared to be damaged and/or dead. The appearance of FC crystals in the medium during prolonged incubation indicated that the cells may either expel crystals or eventually undergo lysis.

A number of morphological studies have demonstrated the involvement of lysosomes in the deposition of cholesterol within foam cells (8, 12). Some of these investigations have illustrated intracellular crystals that have been thought to be cholesterol. However, cholesterol crystals, or clefts, are most prominent in the necrotic core regions present in the intermediate and advanced atheromatous plaque (10, 19). The origin of this extracellular cholesterol remains to be resolved. A number of different possibilities can be suggested. *1)* It has been demonstrated that serum lipoproteins are present within the vessel wall (28–30) and that the concentration of lipoproteins increases as the lesion becomes more necrotic (31). Although these lipoproteins, in their native state, would not have sufficient FC to result in the formation of crystals, the hydrolysis of lipoprotein CE by hydrolases that could be present in the interstitial fluid, together with FC that could be contributed by FC/phospholipid particles that have been observed in the plaque (32), might provide sufficient FC to promote crystallization. *2)* A more likely source of extracellular FC crystals within the vessel would be from the crystallization of cholesterol within the cells of the plaque. Intracellular crystals of cholesterol have been observed in foam cells present in the lesions of hypercholesteromic rabbits (8, 12), and these crystals are localized primarily in lipid-filled, membrane-enclosed structures that have been identified as lysosomes (8, 12). The sequence of events leading to the deposition of cholesterol crystals proposed by Lupu, Danaricu, and Simionescu (12) is consistent with the events that we have documented in the macrophage cell culture system (18). In this system, the engorgement of lysosomes with CE leads to the production of FC, accompanied by the retention of a large fraction of the generated FC within the lysosomes. The quantitative aspects of this FC accumulation have been presented previously (18). When the FC level exceeds the solubility limits of the lipid phase within the lysosome, the FC crystallizes. It is clear from our present study that the formation of a cholesterol crystal within a cell does not rapidly or invariably lead to cell death. Indeed, most of the cells we have observed containing a single crystal appeared viable, and the presence of crystals did not result in an increase in the LDH release to the culture medium. It was only when cells accumulated multiple crystals that clear toxicity was evident. Cholesterol crystals were released from the cells and became more evident in the culture medium as the incubation periods were extended. The extracellular crystals probably arose from cell lysis, but they may also result from an active expulsion from cells. Although we did not observe such a crystal expulsion, we did document the extensive intracellular movement of crystals, with apparent protrusion through the cell membrane (Fig. 4). Using P388D macrophages, McConathy, Koren, and Stiers (33) showed that cholesterol monohydrate crystals can be incorporated by the macrophages.

Numerous studies have been conducted on macrophages in culture that have led to the extensive loading of these cells with large intracellular pools of both free and esterified cholesterol (31, 34–40). However, to our knowledge, the present report is the first to document the extensive presence of cholesterol crystals; thus the formation of these crystals is not the inevitable outcome of cellular FC accumulation. It appears that the primary factor responsible for intracellular cholesterol crystallization is the accumulation of FC within a confined subcellular compartment such as the lysosome. The routine procedure used for loading macrophages in culture with excess cholesterol is through the uptake of modified or abnormal lipoproteins by unregulated receptors such as the scavenger receptor (34, 41). Under these conditions the excess CE is a product of the ACAT reaction and the esters are deposited in cytoplasmic inclusions. It is likely that the excess FC is distributed among cellular membranes where it is solubilized in phospholipid bilayers (10). In contrast, the loading of cells through the phagocytosis of CE droplets delivers a large bolus of CE directly into the lysosomal compartment, resulting in the generation of FC in excess of that which can be removed (18). The more regulated receptor-mediated uptake of CE as a component of lipoproteins probably would distribute the CE among a much larger population of lysosomes and thus not normally result in lysosomal CE overloading, with subsequent cholesterol crystallization.

If the rapid delivery of large amounts of cholesterol to a limited population of lysosomes was responsible for the accumulation, and subsequent crystallization of FC, then a number of extracellular particles can be implicated. We have previously proposed that cytoplasmic CE inclusions initially formed in macrophage-derived foam cells could be liberated by lysis and then recycled into both newly recruited macrophages and/or smooth muscle cells (15, 17). We have now shown that such inclusions are incorporated by cells in culture (15–17) and that the FC generated

in the lysosomes is retained (18) and forms crystals. Other extracellular particles could also produce the same series of events in cells within the vessel wall. For example, aggregates of lipoproteins (39, 42, 43), lipoprotein complexes with extracellular matrix material (39, 44), or mast cell granules coated with LDL (45), all might produce the type of CE delivery necessary for the resultant cholesterol crystal formation. In addition to the delivery of extracellular particles, we have obtained evidence that the intracellular CE inclusions formed by the action of ACAT can, under some conditions, be directed into lysosomes of macrophages (J. M. Glick, unpublished observations). If

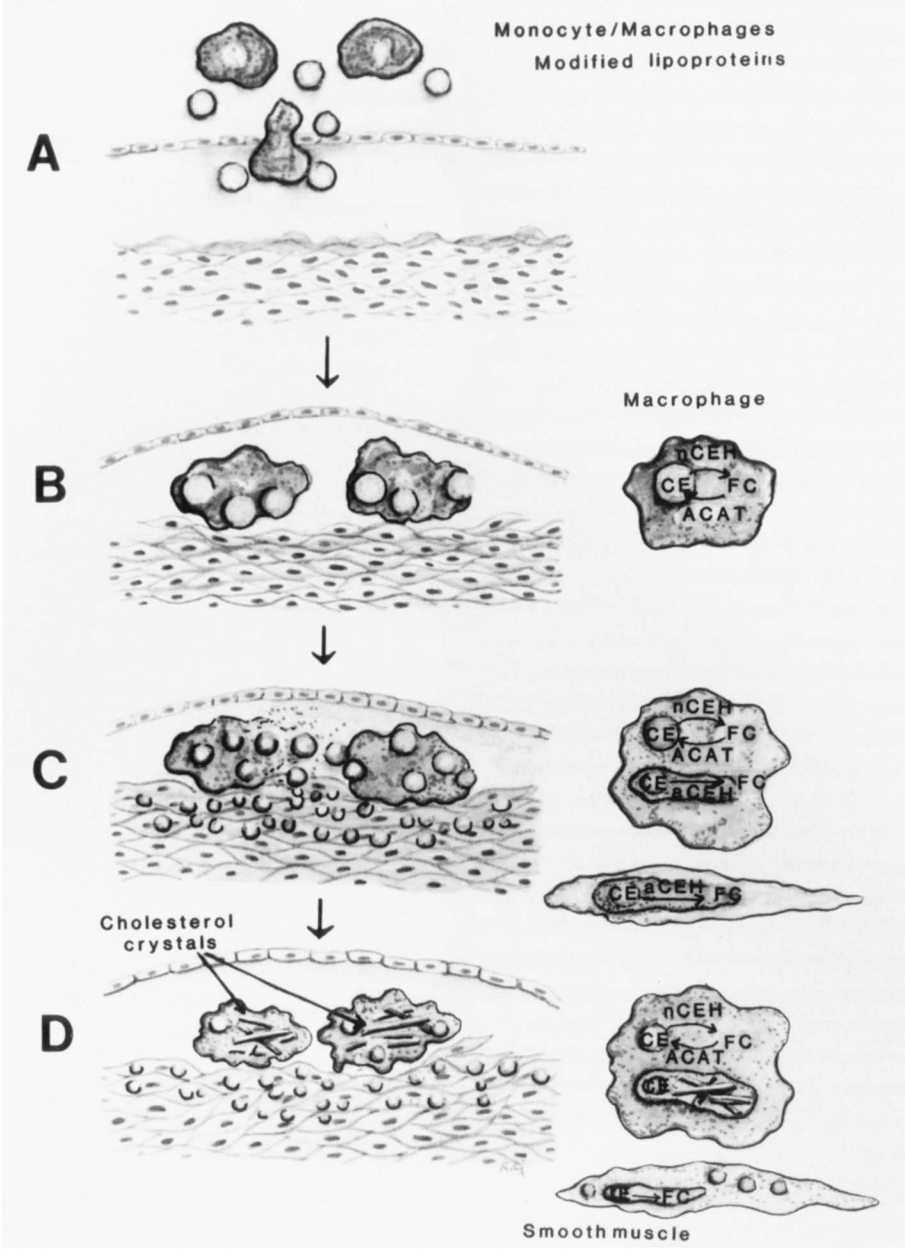

Fig. 7. A model for the recycling of CE droplets and cholesterol accumulation in foam cells during progression of atherosclerosis. A) Infiltration of circulating monocytes into the arterial wall followed by the incorporation of excess cholesterol from modified lipoproteins by the monocyte/macrophages could lead to the formation of earliest macrophage-derived foam cells. B) In the early lesions, the foam cells are primarily macrophage-derived foam cells with the cholesterol deposited primarily as cytoplasmic inclusions. C) Progression of the lesion would lead to the lysis of some early foam cells with the liberation of CE inclusions. The phagocytic incorporation of the liberated inclusions by macrophages leads to lysosomal CE hydrolysis by the action of acid cholesteryl ester hydrolase (aCEH) with the generation of FC. Rapid CE hydrolysis and FC accumulation in the macrophage-foam cells results in FC deposition in the lipid-filled lysosomes. D) The accumulation of FC in the lipid-filled lysosomes of macrophage foam cells leads to the formation of cholesterol monohydrate crystals. The formation of FC crystals could eventually result in the lysis and death of the cells.

this internal recycling takes place, it is probable that lysosomal FC accumulation would occur with the ultimate result being the production of cholesterol monohydrate crystals. The series of events that may happen within the vessel wall that result in the accumulation of both FC and EC in foam cell lipid inclusions and lysosomes and the formation of crystal is presented in **Fig. 7.** As it is now possible, with the experimental systems described in this paper, to produce intracellular crystals, we will now be able to test details of this model, such as the factors regulating the crystallization in specific cells, the effect of crystals on cell functions, the mechanisms responsible for crystal release from cells, and the mobilization of crystalline cholesterol upon the initiation of cholesterol efflux.

We are grateful to Dr. Michael C. Phillips for helpful comments and discussion, to Dr. Nina S. Allen for use of her video microscopy facility at Wake Forest University, and to Marie Plyler for technical support. This work was supported in part by Program Project grants HL-22633, HL-26335, and Training Grant HL-07443 from the National Heart, Lung, and Blood Institute of the National Institutes of Health, American Heart Association predoctoral fellowship, Southeastern Pennsylvania affiliate (RKT), and American Heart Association Grant-in-Aid 900709.

Manuscript received 7 May 1993 and in revised form 19 August 1993.

REFERENCES

1. Lewis, J. C., R. G. Taylor, and W. G. Jerome. 1985. Foam cell characteristics in coronary arteries and aortas of White Carneau pigeons with moderate hypercholesterolemia. *Ann. N. Y. Acad. Sci.* **454:** 91–100.
2. Rosenfeld, M. E., T. Tsukada, A. Chait, E. L. Bierman, A. M. Gown, and R. Ross. 1987. Fatty streak expansion and maturation in Watanabe heritable hyperlipemic and comparably hypercholesterolemic fat-fed rabbits. *Arteriosclerosis.* **7:** 24–34.
3. Rosenfeld, M. E., T. Tsukada, A. M. Gown, and R. Ross. 1987. Fatty streak initiation in Watanabe heritable hyperlipemic and comparably hypercholesterolemic fat-fed rabbits. *Arteriosclerosis.* **7:** 9–23.
4. Jerome, W. G., and J. C. Lewis. 1987. Early atherogenesis in the White Carneau pigeon. III. Lipid accumulation in nascent foam cells. *Am. J. Pathol.* **128:** 253–264.
5. Shio, H., N. J. Haley, and S. Fowler. 1978. Characterization of lipid-laden aortic cells from cholesterol-fed rabbits. II. Morphometric analysis of lipid-filled lysosomes and lipid droplets in aortic cell population. *Lab. Invest.* **39:** 390–397.
6. Jerome, W. G., and J. C. Lewis. 1985. Early atherogenesis in White Carneau pigeons. II. Ultrastructural and cytochemical observations. *Am. J. Pathol.* **119:** 210–222.
7. Lewis, J. C., R. G. Taylor, and K. Ohta. 1988. Lysosomal alterations during coronary atherosclerosis in the pigeon: correlative cytochemical and three-dimensional HVEM/IVEM observations. *Exp. Mol. Pathol.* **48:** 103–115.
8. Shio, H., N. J. Haley, and S. Fowler. 1979. Characterization of lipid-laden aortic cells from cholesterol-fed rabbits. III. Intracellular localization of cholesterol and cholesteryl ester. *Lab. Invest.* **41:** 160–167.
9. Stary, H. C. 1991. The sequence of cell and matrix changes in atherosclerotic lesions of coronary arteries in the first forty years of life. *Eur. Heart J.* **11:** 3–19.
10. Small, D. M. 1988. Progression and regression of atherosclerotic lesions. *Arteriosclerosis.* **8:** 103–129.
11. Small, D. M. 1977. Cellular mechanisms for lipid deposition in atherosclerosis. *N. Engl. J. Med.* **297:** 873–877.
12. Lupu, F., I. Danaricu, and N. Simionescu. 1987. Development of intracellular lipid deposits in the lipid-laden cells of atherosclerotic lesions. *Atherosclerosis.* **67:** 127–142.
13. Guyton, J. R., and K. F. Klemp. 1989. The lipid-rich core region of human atherosclerotic fibrous plaques. *Am. J. Pathol.* **134:** 705–717.
14. Bocan, T. M. A., and J. R. Guyton. 1985. Human aortic fibrolipid lesions: progenitor lesions for fibrous plaques, exhibiting early formation of the cholesterol-rich core. *Am. J. Pathol.* **120:** 193–206.
15. Wolfbauer, G., J. M. Glick, L. K. Minor, and G. H. Rothblat. 1986. Development of the smooth muscle foam cell: uptake of macrophage lipid inclusions. *Proc. Natl. Acad. Sci. USA.* **83:** 7760–6664.
16. Minor, L. K., G. H. Rothblat, and J. M. Glick. 1989. Triglyceride and cholesteryl ester hydrolysis in a cell culture model of smooth muscle foam cells. *J. Lipid Res.* **30:** 189–197.
17. Mahlberg, F. H., J. M. Glick, W. G. Jerome, and G. H. Rothblat. 1990. Metabolism of cholesteryl ester lipid droplets in a J774 macrophage foam cell model. *Biochim. Biophys. Acta.* **1045:** 291–298.
18. Tangirala, R. K., F. H. Mahlberg, J. M. Glick, W. G. Jerome, and G. H. Rothblat. 1993. Lysosomal accumulation of unesterified cholesterol in model macrophage foam cells. *J. Biol. Chem.* **268:** 9653–9660.
19. Small, D. M., and G. G. Shipley. 1974. Physical-chemical basis of lipid deposition in atherosclerosis. *Science.* **185:** 222–229.
20. Bernard, D. W., A. Rodriguez, G. H. Rothblat, and J. M. Glick. 1990. Influence of high density lipoprotein on esterified cholesterol stores in macrophages and hepatoma cells. *Arteriosclerosis.* **10:** 135–144.
21. Berstein, L. H., and J. Everse. 1975. Determination of the isoenzyme levels of lactate dehydrogenase. *Methods Enzymol.* **41:** 47–52.
22. Dey, C. S., and G. C. Majumder. 1988. A simple quantitative method of estimation of cell-intactness based on ethidium bromide florescence. *Biochem. Int.* **17:** 367–374.
23. Allen, R. D. 1985. New observations on cell architecture and dynamics by video-enhanced contrast optical microscopy. *Annu. Rev. Biophys. Chem.* **14:** 265–290.
24. Jerome, W. G., L. K. Minor, J. M. Glick, G. H. Rothblat, and J. C. Lewis. 1991. Lysosomal lipid accumulation in vascular smooth muscle cells. *Exp. Mol. Pathol.* **540:** 144–158.
25. Gomori, G. 1952. Microscopic Histochemistry: Principles and Practice. University of Chicago Press, Chicago.
26. Loomis, C. R., G. G. Shipley, and D. M. Small. 1979. The phase behavior of hydrated cholesterol. *J. Lipid Res.* **20:** 525–535.
27. Katz, S. S., and D. M. Small. 1980. Isolation and partial characterization of the lipid phases of human atherosclerotic plaques. *J. Biol. Chem.* **255:** 9753–9759.
28. Stender, S., and D. B. Zilversmit. 1981. Transfer of plasma lipoprotein components and of plasma proteins into aortas of cholesterol-fed rabbits; molecular size as a determinant of plasma lipoprotein influx. *Arteriosclerosis.* **1:** 38–49.

29. Schwenke, D. C., and T. E. Carew. 1989. Initiation of atherosclerotic lesions in cholesterol-fed rabbits. I. Local increases in arterial LDL concentration precede development of fatty streak lesions. *Arteriosclerosis.* **9:** 895–907.
30. Frank, J. S., and A. M. Fogelman. 1989. Ultrastructure of the intima in WHHL and cholesterol-fed rabbit aortas prepared by ultra-rapid freezing and freeze-etching. *J. Lipid Res.* **30:** 967–978.
31. Hoff, H. F., J. O'Neil, J. M. Pepin, and T. B. Cole. 1990. Macrophage uptake of cholesterol-containing particles derived from LDL and isolated from atherosclerotic lesions. *Eur. Heart J.* **11:** 105–115.
32. Kruth, H. S. 1985. Subendothelial accumulation of unesterified cholesterol: an early event in atherosclerotic lesion development. *Atherosclerosis.* **57:** 337–341.
33. McConathy, W. J., E. Koren, and D. L. Stiers. 1989. Cholesterol crystal uptake and metabolism by P388D macrophages. *Atherosclerosis.* **77:** 221–225.
34. Brown, M. S., and J. L. Goldstein. 1983. Lipoprotein metabolism in the macrophage: implications for cholesterol deposition in atherosclerosis. *Annu. Rev. Biochem.* **52:** 223–261.
35. Ho, Y. K., M. S. Brown, and J. L. Goldstein. 1980. Hydrolysis and excretion of cytoplasmic cholesteryl esters by macrophages: stimulation by high density lipoprotein and other agents. *J. Lipid Res.* **21:** 391–398.
36. Fogelman, A. M., I. Shecter, J. Seager, M. Hokom, J. S. Child, and P. A. Edwards. 1980. Malondialdehyde alteration of low density lipoproteins leads to cholesteryl ester accumulation in human monocyte-macrophages. *Proc. Natl. Acad. Sci. USA.* **77:** 2214–2218.
37. Mahley, R. W., T. L. Innerarity, M. S. Brown, Y. K. Ho, and J. L. Goldstein. 1980. Cholesteryl ester synthesis in macrophages: stimulation by β-very low density lipoproteins from cholesterol-fed animals of several species. *J. Lipid Res.* **21:** 970–980.
38. McGookey, D. J., and R. G. W. Anderson. 1983. Morphological characterization of the cholesteryl ester cycle in cultured mouse macrophage foam cells. *J. Cell Biol.* **97:** 1156–1168.
39. Falcone, D. J., N. Mated, H. Shio, C. R. Minick, and D. Fowler. 1984. Lipoprotein-heparin-fibronectin-denatured collagen complexes enhance cholesteryl ester accumulation in macrophages. *J. Cell Biol.* **99:** 1266–1274.
40. Via, D. P., A. L. Plant, I. F. Craig, A. M. Gotto, and L. C. Smith. 1985. Metabolism of normal and modified low-density lipoproteins by macrophage cell lines of murine and human origin. *Biochim. Biophys. Acta.* **833:** 417–428.
41. Goldstein, J. L., Y. K. Ho, S. K. Basu, and M. S. Brown. 1979. Binding site on macrophages that mediates uptake and degradation of acetylated low density lipoprotein, producing massive cholesterol deposition. *Proc. Natl. Acad. Sci. USA.* **76:** 333–337.
42. Suits, A. G., A. Chait, M. Aviram, and J. W. Heinecke. 1989. Phagocytosis of aggregated lipoprotein by macrophages: low density lipoprotein receptor-dependent foam-cell formation. *Proc. Natl. Acad. Sci. USA.* **86:** 2713–2717.
43. Khoo, J. C., E. Miller, P. McLaughlin, and D. Steinberg. 1988. Enhanced macrophage uptake of low density lipoprotein after self-aggregation. *Arteriosclerosis.* **8:** 348–358.
44. Vijayagopal, P., S. R. Srinivasan, K. M. Jones, B. Radhakrishnamurthy, and G. S. Berenson. 1985. Complexes of low-density lipoproteins and arterial proteoglycan aggregates promote cholesteryl ester accumulation in mouse macrophages. *Biochim. Biophys. Acta.* **837:** 251–261.
45. Kovanen, P. T. 1991. Mast cell granule-mediated uptake of low density lipoproteins by macrophages: a novel carrier mechanism leading to the formation of foam cells. *Ann. Med.* **23:** 551–559.